SCA2003-33: MEASUREMENT OF RELEVANT GAS CONDENSATE RELATIVE PERMEABILITY DATA FOR WELL DELIVERABILITY PREDICTIONS FOR A DEEP MARINE SANDSTONE RESERVOIR

P. Ayyalasomayajula, N. Silpngarmlers, J. Berroteran, J. Sheffield, and J. Kamath
(ChevronTexaco)

This paper was prepared for presentation at the International Symposium of the Society of Core Analysts held in Pau, France, 21-24 September 2003

ABSTRACT

Fevang and Whitson[1] have shown that the appropriate data for well deliverability predictions in gas condensate reservoirs are k_{rg} = f (k_{rg}/k_{ro}, Nc). However, there is very little published data of this form. We present an extensive data set on four rock samples from a deep marine sandstone reservoir. These data span the k_{rg}/k_{ro} and capillary number parameter space. We discuss the issues behind the design of the experiments and also results of numerical simulation of these specialized corefloods. The data measured on these samples are then compared with the sparse published data set. Finally, we use the measured data and detailed geological information to demonstrate the impact of relative permeability data on prediction of well performance in this reservoir.

APPROPRIATE DATA FOR WELL DELIVERABILITY

Fevang and Whitson[1] have demonstrated that $k_{rg} = f(k_{rg}/k_{ro}, N_c)$ is the underlying relative permeability relationship determining well deliverability of gas condensate reservoirs. They have shown that the condensate saturation near the well does not play a significant role as long as the functional relationship between k_{rg} vs. k_{rg}/k_{ro} remains the same. They have also confirmed this by performing rate-time studies of a gas condensate reservoir using two different sets of relative permeabilities with completely different $k_{rg}(S_g)$ and $k_{ro}(S_g)$ curves, but with an identical $k_{rg} = f(k_{rg}/k_{ro})$ relationship. Both sets of relative permeabilities yielded identical well performance. They have also shown that the ratio k_{rg}/k_{ro} is a function of the saturated oil and gas PVT properties, which are dependent on pressure only. These observations are very significant as it is not necessary to measure saturation, and appropriate experiments can be conducted very simply and rapidly.

EXPERIMENTAL SET-UP AND PROCEDURE

A high -pressure core flow apparatus (Figure 1) was built to conduct steady-state relative permeability measurements of gas condensates. The experiments have been designed so as to capture the key aspects of the flow near the well. The two most important aspects of the experiments are (i) they define the $k_{rg} = f(k_{rg}/k_{ro})$ for the range of k_{rg}/k_{ro} values that would be expected in a well and (ii) they allow for measurements at a range of flow rates so as to quantify the capillary number effects.

A large cylinder (II) contains an equilibrium synthetic gas, which has properties similar to the original reservoir fluid. The properties of this fluid are given in more detail in the PVT section of this study. The pump (I) supplies equilibrium dew-point gas from the cylinder to the inlet of the core (IV) by flashing it across the upstream back pressure regulator (III). The upstream back pressure regulator is held at the reservoir pressure and the downstream backpressure regulator (V) is set to the bottom hole pressure thus resulting in a two-phase condensate flow across the core. The pressure drop and the flow rate are noted after steady state conditions are achieved. The pump rate is then changed and the test is now repeated at a different capillary number. This results in the k_{rg} variation with capillary number (N_c) at a fixed k_{rg}/k_{ro}. The gas in the cylinder is then bled off until the pressure in the tank drops to a lower reservoir pressure and the above procedure is repeated to yield the same data at a different k_{rg}/k_{ro} value.

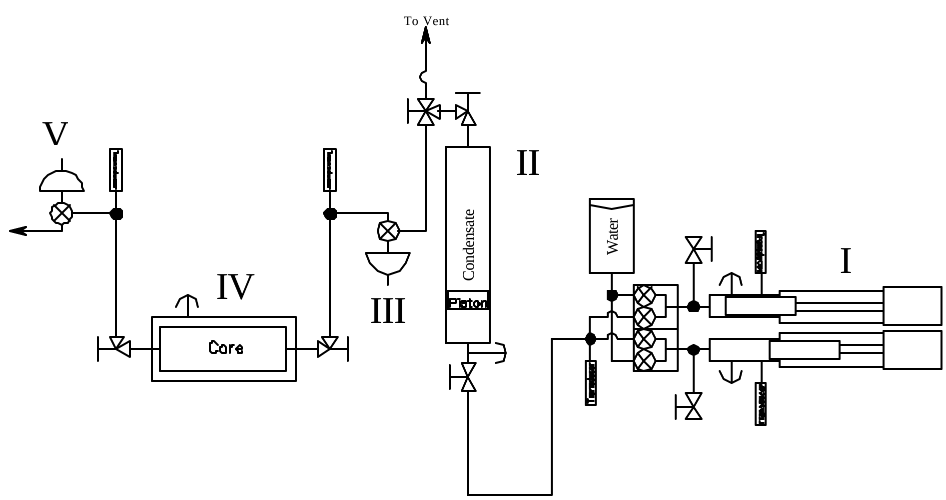

Figure 1: Schematic diagram of core flow apparatus for gas condensate systems

CORE SAMPLES

The Miocene shoreface core samples used in the experiments are 2″ long and 1.5″ in diameter. The samples are miscibly cleaned and the permeability is measured. The samples are then saturated with brine and spun in a centrifuge to S_{wi}. The sample properties are listed in Table 1.

Table 1: Core sample properties

ϕ (%)	K (mD)	S_{wi}
10.1	51	9
13	15	12
-	5	-
9.5	3	20

The rocks have similar pore size distribution. Figure 2 shows typical thin section images of two different rocks and Figure 3 shows the normalized pore throat radius distribution of four different rock samples from this reservoir.

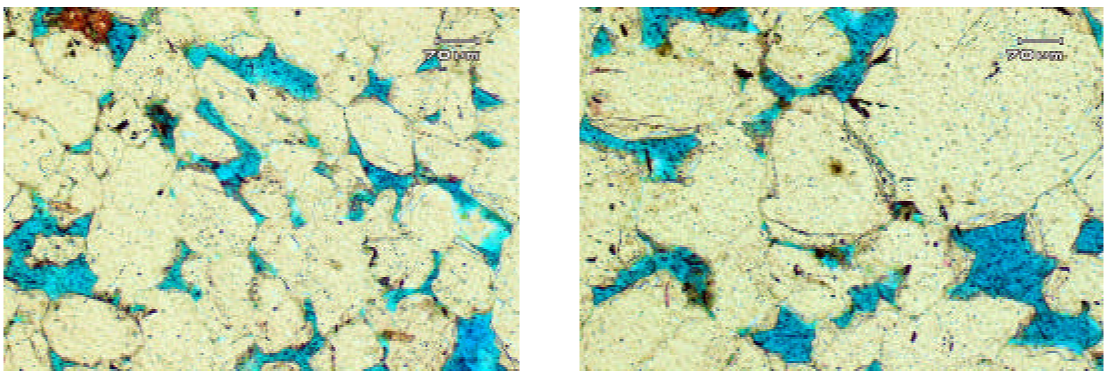

(A) (B)

Figure 2: Thin sections image of two different rock samples

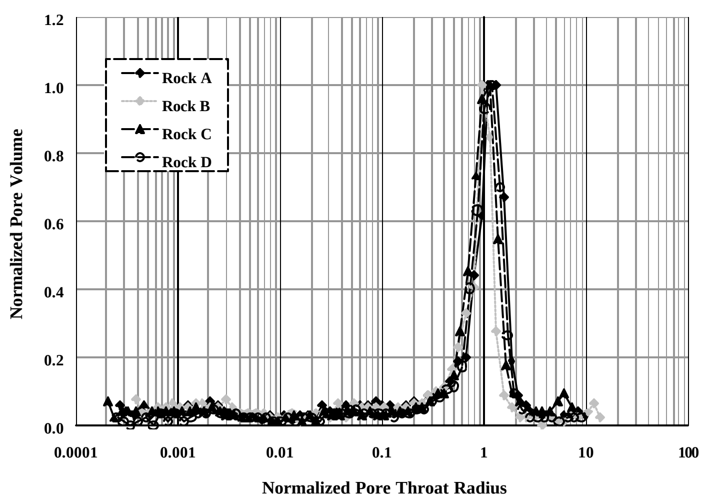

Figure 3: Pore throat radius distribution of the rock samples

FLUID PROPERTIES

Fevang and Whitson[1] have shown the relation between k_{rg}/k_{ro} and fluid properties as

$$k_{rg}/k_{ro} = (1/V_{ro}-1)*\mu_g/\mu_o, \qquad (1)$$

where V_{ro} is the relative oil volume from a Constant Composition Expansion (CCE) and μ_g/μ_o is the ratio of the gas and oil viscosity of the steady state flowing phases in the near wellbore region.

The reservoir gas condensate is a relatively lean fluid (46 STB/MMSCF) with a dew point pressure of 6490 psia at the reservoir temperature of 290°F. A three -component synthetic gas condensate fluid was developed for the laboratory corefloods. The synthetic gas condensate was designed with the objective of reasonably matching the V_{ro} and μ_g/μ_o behavior of the reservoir gas condensates, while operating the corefloods at a much lower temperature than reservoir temperature (120°F vs 290°F).

Oil Viscosity. Oil viscosity is a critical parameter for well deliverability predictions. The Lohrenz-Bray-Clark (LBC) correlation[2] is used in our EOS software to calculate the oil and gas phase viscosity. The LBC correlation does a good job of predicting the gas phase viscosity but must be optimized to calculate the oil phase viscosity. A three component EOS model was developed for the synthetic gas condensate that matched the CCE data and used to predict the composition of a "typical" liquid phase flowing during a steady state coreflood. The calculated liquid phase composition was synthesized and the viscosity of the liquid was measured in a capillary tube viscometer. This viscosity was used to optimize the three component EOS model.

Table 2 lists the composition of the reservoir and synthetic fluids. Figure 4 compares the liquid dropout curves and viscosity ratio from a CCE of the reservoir and synthetic gas condensates.

Table2: Fluid compositions of the reservoir and synthetic gas condensates, and synthetic liquid used for viscosity measurement

Component	Reservoir Gas Condensate mole %	Component	Synthetic Gas Condensate mole %	Synthetic Liquid mole %
CO2	3.69	METHANE	98.70	61.07
N2	0.06	N-C10	0.98	22.68
METHANE	83.31	N-C20	0.32	16.25
ETHANE	3.88	Total	100.00	100.00
PROP	3.13			
I-C4	1.30			
N-C4	1.01			
I-C5	0.42			
N-C5	0.26			
C6	0.27			
C7	0.25			
C8	0.34			
C9	0.40			
C10	0.55			
C11	0.24			
C12+	0.89			
Total	100.00			
C7+ Mole %	2.67			
C7+ Mole Wt	170			

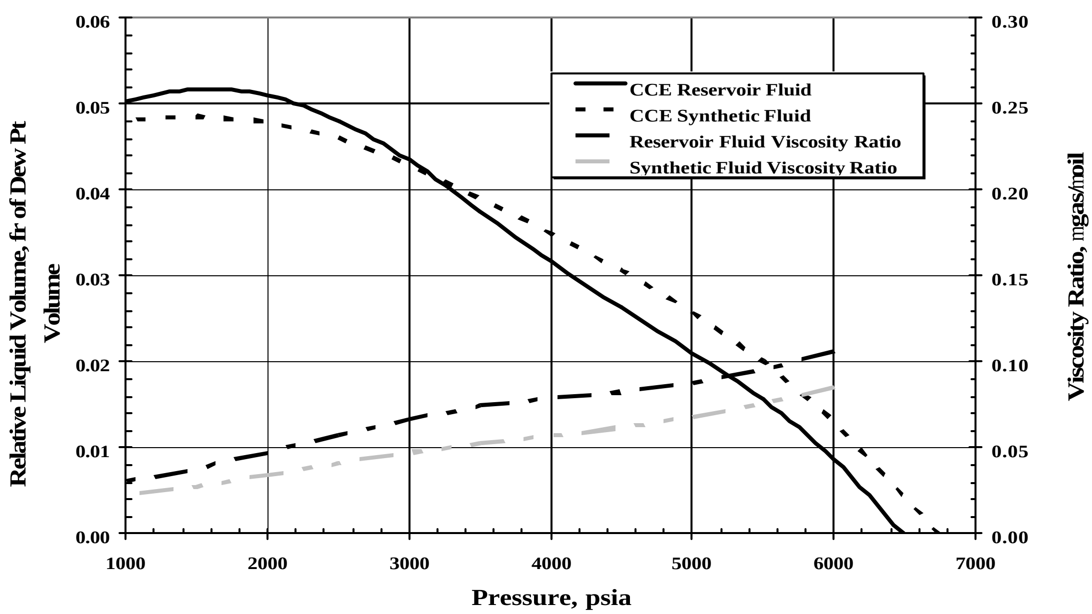

Figure 4: Liquid volume fraction curves and viscosity ratios for synthetic and reservoir fluid

Figure 5 shows the range of expected k_{rg}/k_{ro} in region 1 (described in Ref. [1]) in the reservoir. These plots have been generated from the experimentally measured viscosity using Equation (1). All the experimental data are measured in this k_{rg}/k_{ro} range of interest, i.e. from 1 to 50. We also note that the surface tensions in the reservoir fluid is of the order of 30 dynes/cm and that of the synthetic fluid is of the order of 15 dynes/cm

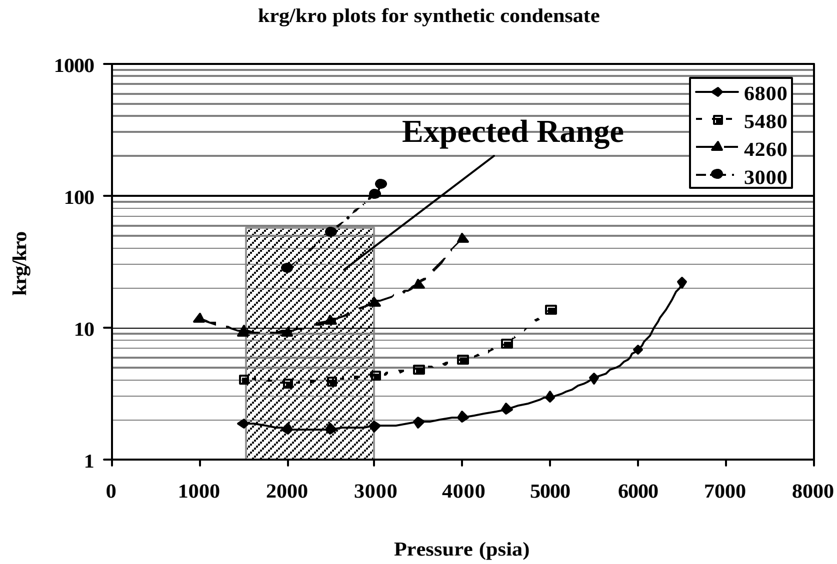

Figure 5: k_{rg}/k_{ro} as a function of core pressure for synthetic gas condensate

RELATIVE PERMEABILITY MEASUREMENTS

Figure 6 shows a typical rate versus pressure drop data measured during the relative permeability experiments. The pressure drop is measured as a function of pore volumes flowed until it stabilizes. The pump rate is then increased to a new capillary number value and the process is repeated. We observe that the pressure drop stabilizes typically after about 15 to 20 pore volumes.

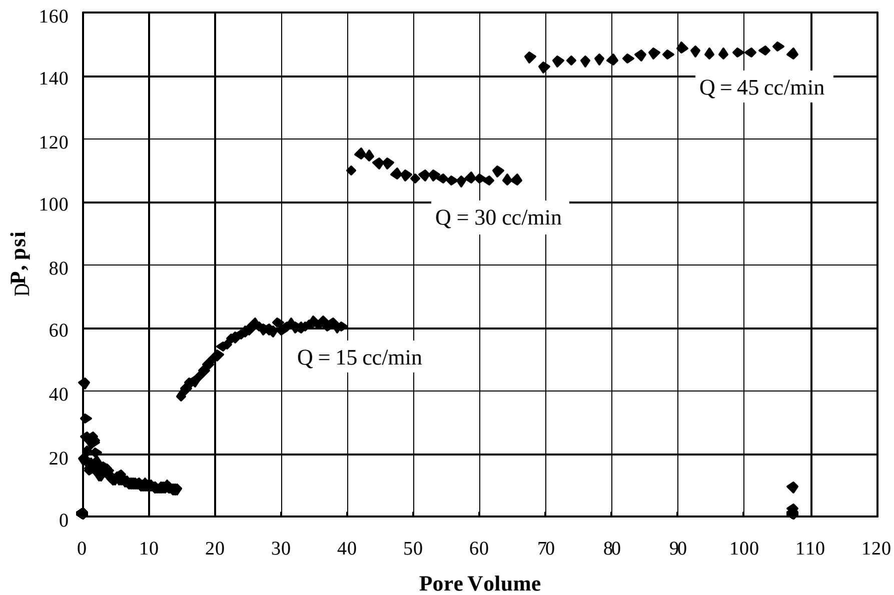

Figure 6: Pressure drop across the core for 3 mD rock at a k_{rg}/k_{ro} of 40.2 (cylinder pressure = 2700 psi, core pressure = 1500 psi)

The experimental relative permeability data of the 4 rocks in this study are presented in Figures 7(a) through 7(d). Figure 7(d) also compares the measured data on the 15 mD rock with a North Sea[3] rock with absolute permeability of 20 mD. It is observed that the rocks in this study have lower k_{rg} than the North Sea samples. Figure 8 shows the plot of gas relative permeability of the four rocks as a function of capillary number at a given k_{rg}/k_{ro} value. The data suggest that the gas relative permeability is independent of the absolute permeability of the rock for a given k_{rg}/k_{ro} within the given experimental error limits. This could be due to the similarity in the pore throat radius distribution of the rocks as illustrated in Figure 3.

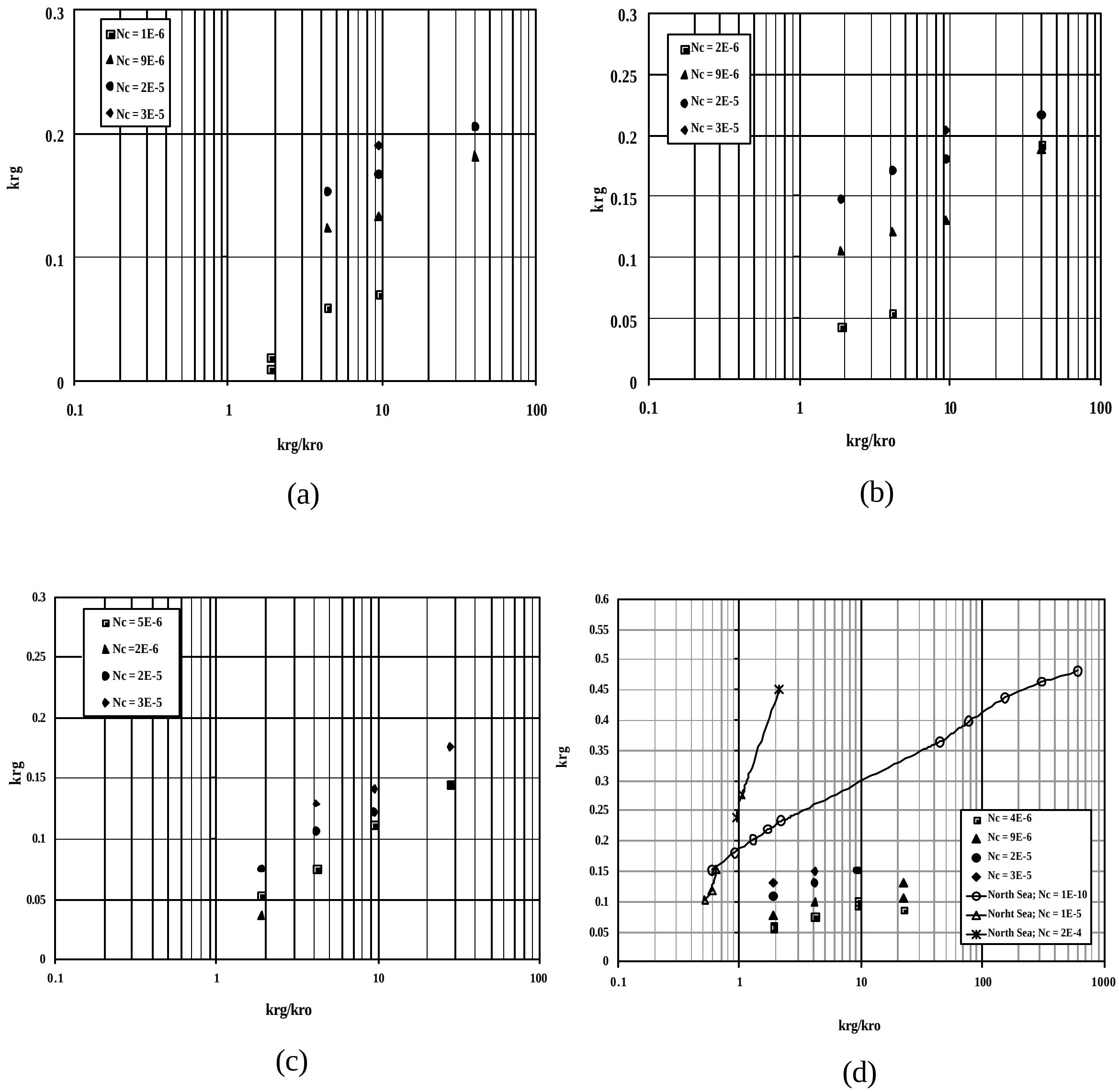

Figure 7: Measured k_{rg} vs k_{rg}/k_{ro} at different capillary numbers of the four rocks; (a) 3 mD rock; (b) 5 mD rock; (c) 50 mD rock; (d) 15 mD rock and comparison with North Sea data

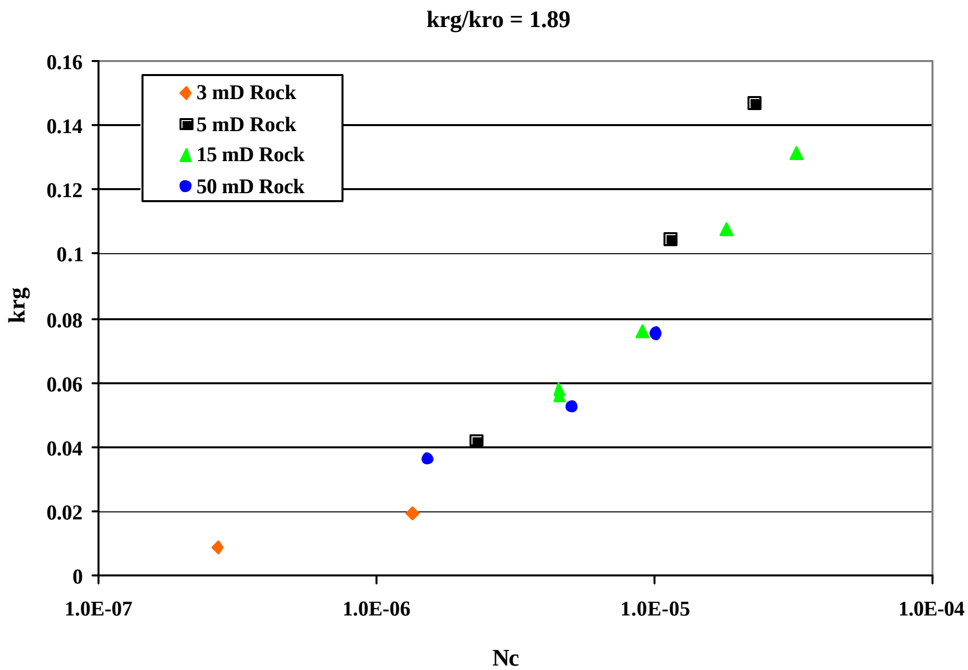

Figure 8: Comparison of k_{rg} vs Nc of different rocks for k_{rg}/k_{ro} at 1.89

SIMULATION STUDIES

Coreflood Simulation

Numerical simulations of the coreflood experiment are performed to investigate the capillary end effect. A schematic diagram of the 1-D system used in coreflood simulation is shown in Figure 9.

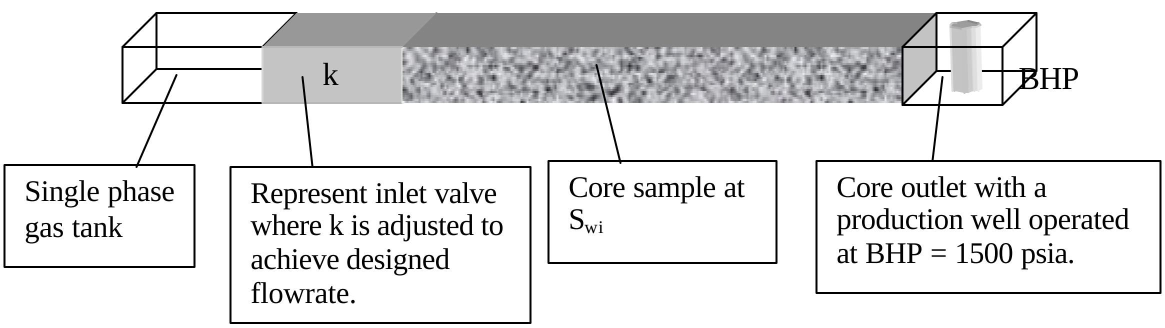

Figure 9: A schematic diagram of the system used in coreflood simulation

Numerical simulations are performed for 15 mD rock to simulate the coreflood experiments at 6800 psia and 3068 psia with the core backpressure of 1500 psia. These pressures correspond to k_{rg}/k_{ro} of 1.89 and 22.5, respectively. The simulations are initially conducted without taking into account the capillary pressure. Then, the runs are repeated with the incorporation of capillary pressure data shown in Figure 10. The simulation results in the form of $k_{rg} = f(k_{rg}/k_{ro}, Nc)$ are compared between the cases with and without capillary pressure as shown in Figure 11. The comparison shows no differences in relative permeability values in the presence of capillary pressure for $k_{rg}/k_{ro} = 1.89$. At a higher k_{rg}/k_{ro}, i.e. $k_{rg}/k_{ro} = 22.5$, a slight discrepancy in relative permeability values is observed. This difference, however, is negligibly small.

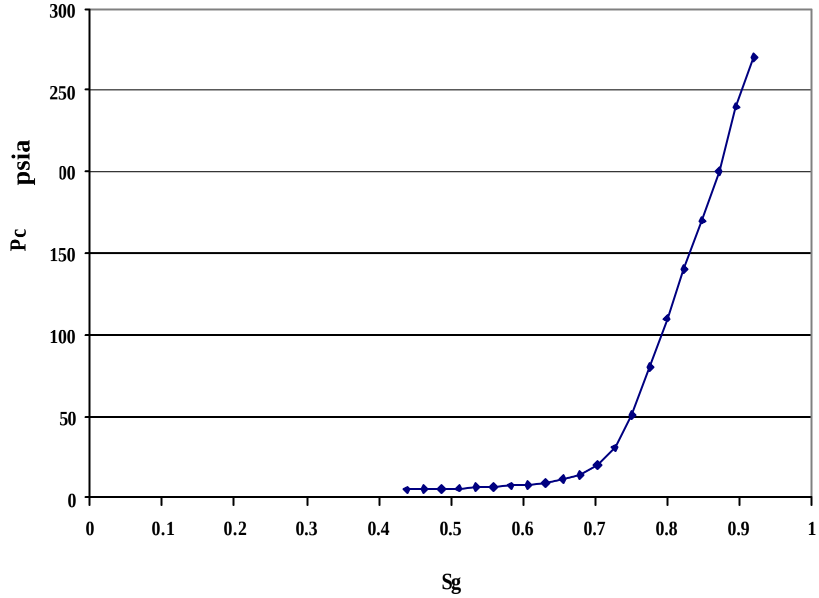

Figure 10: Capillary pressure data used in coreflood simulation obtained by mercury injection method

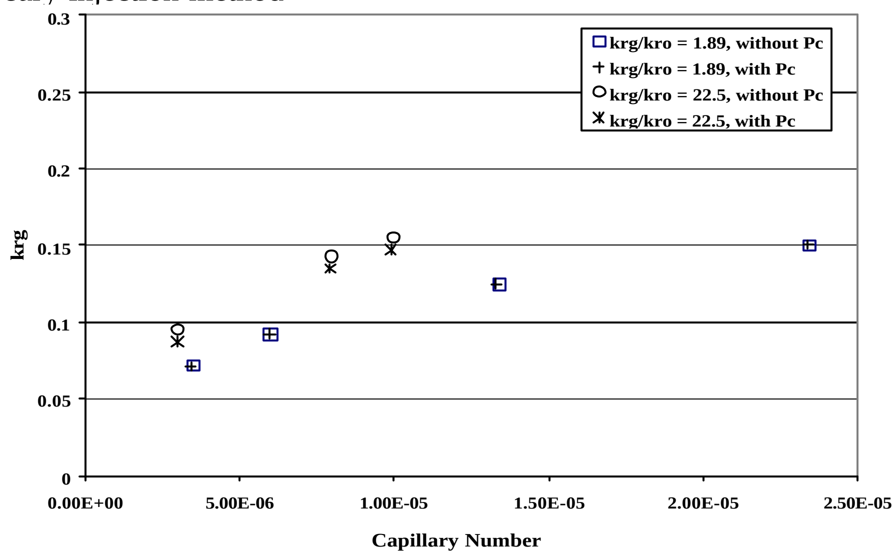

Figure 11: Comparison of results from coreflood simulations

EFFECT OF RELATIVE PERMEABILITY ON WELL PERFORMANCE

Effect of relative permeability on the well deliverability is investigated by conducting compositional simulations using a single well model in which the well is produced at a constant flowrate. In order to capture the flow performance near the well, the grid blocks near the well are refined. The reservoir description is shown in Table 3.

Table 3: Reservoir description

P_{int} = 6515 psia	Porosity(avg.) = 9 %	Max. Q_{gas} = 20 MMSCFD
Area = 8900 x 7760 ft^2	Permeability(avg.) =22 mD	Min. BHP = 2300 psia
Thickness = 171 ft	Temperature = 290 F	

Simulation models need $k_{rg} = f(S_g)$. We fit the measured data using a model such as the one described by Whitson[3]. Figure 12 shows the $k_r(S_g)$ data used in simulations.

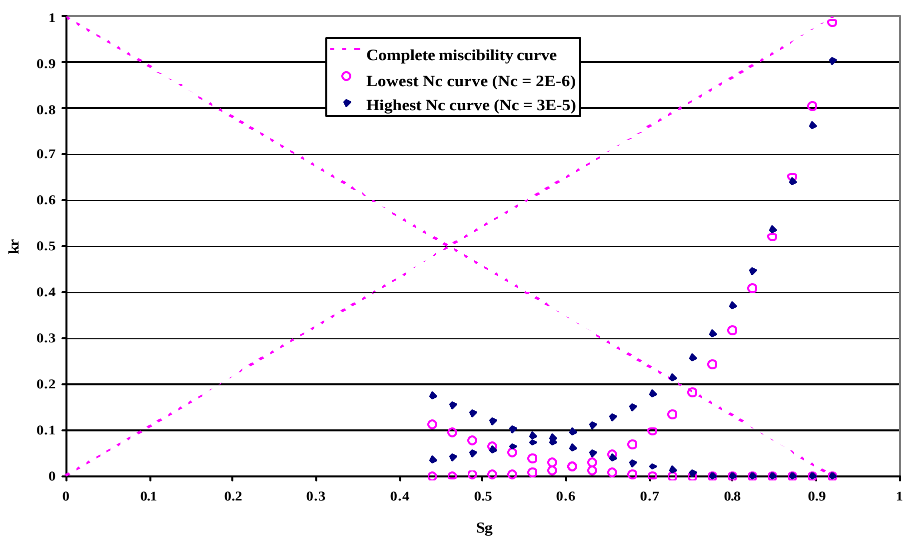

Figure 12: Gas-oil relative permeability data sets used in simulations.

The normalized PI+ obtained from using different relative permeability data are plotted for comparison in Figure 13. The comparison shows the decrease in PI of approximately 10% in the case of no condensate blockage. This is due to transient effects. Figure 13 shows that for the case in which relative permeability varies with capillary number, there is a sharp decrease in PI initially. The PI then continues to decline gradually from approximately two years until 17 years. The well again experiences another decline in PI which is attributed to the change in well specifications.

+ Initial PI is defined as the PI calculated after the well has been on production for 24 hours

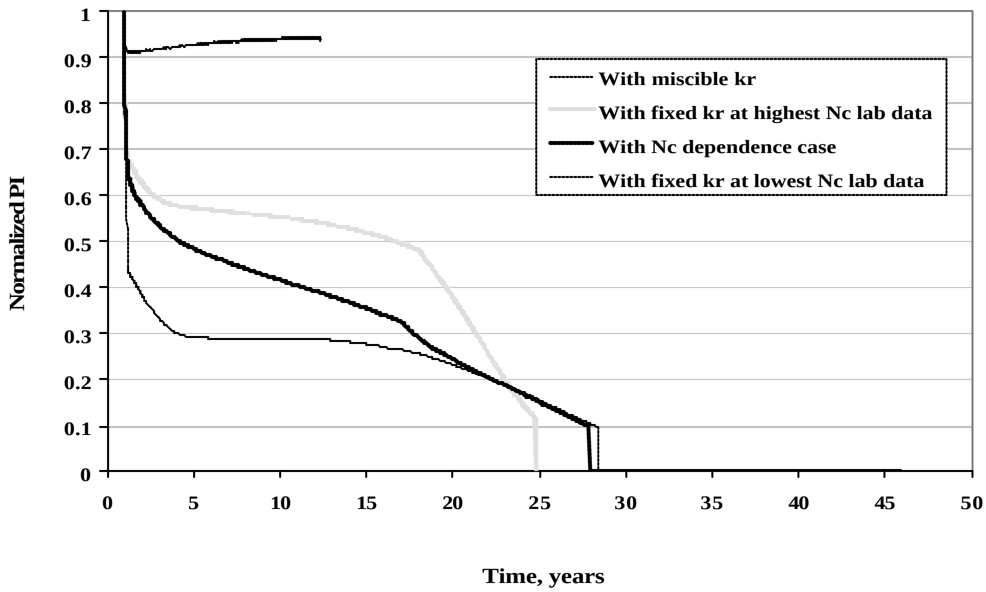

Figure 13: Comparison of normalized PI obtained using different relative permeability data.

SUMMARY

In this work, we have designed and conducted experiments to measure the relevant gas-oil relative permeability data for gas condensate reservoirs. These experiments are intended to measure the appropriate data for well deliverability calculations, including the capillary number effects. We observe that the characteristics of relative permeability measured are similar for the rock types studied. This is due to similar pore size distribution. We have found that relative permeability has significant influence on the well productivity as is shown by the significant reduction in PI when the experimentally measured data is used for well deliverability predictions in the single well model simulations.

NOMENCLATURE

k_r	=	relative permeability		
N_C	=	capillary number	=	$\frac{mv}{s}$
S	=	saturation		
V_{ro}	=	relative oil volume		
m	=	fluid viscosity		
s	=	interfacial tension		
v	=	superficial velocity		

Subscript

c	=	critical
g, o, w	=	gas, oil, water
i	=	initial
r	=	residual

ACKNOWLEDGEMENTS

We thank Stan Franklin for supporting this work. We also thank Frank Nakagawa for assistance with the experimental measurements, and John Popek for providing thin section images.

REFERENCES

1) Fevang, O., Whitson C.H., "Modeling Gas Condensate Well Deliverability," *Paper SPE 30714, presented at the SPE Annual Technical Conference and Exhibition, Dallas, TX* (October 22-25, 1995).

2) Lohrenz, J., Bray, B., and Clark, C. R.: American Institute of Mining, Metallurgical, and Petroleum Engineers. Transactions 231, 1171 (1964).

3) Whitson C.H., Fevang, O., and Saevareid A., "Gas Condensate Relative Permeability for Well Calculations," Paper *SPE 56476*, *presented at the SPE Annual Technical Conference and Exhibition, Houston, TX* (October 3-6, 1999).